



ELSEVIER

Journal of Chromatography A, 828 (1998) 83–90

JOURNAL OF  
CHROMATOGRAPHY A

## Performance of an octadecylsilylated continuous porous silica column in polypeptide separations

Hiroyoshi Minakuchi<sup>a</sup>, Norio Ishizuka<sup>a</sup>, Kazuki Nakanishi<sup>a</sup>, Naohiro Soga<sup>a</sup>,  
Nobuo Tanaka<sup>b,\*</sup>

<sup>a</sup>Kyoto University, Department of Material Chemistry, Graduate School of Engineering, Yoshida, Sakyo-ku, Kyoto 606-8501, Japan

<sup>b</sup>Kyoto Institute of Technology, Department of Polymer Science and Engineering, Matsugasaki, Sakyo-ku, Kyoto 606-8585, Japan

### Abstract

A continuous porous silica rod column prepared by an alkoxy-derived sol-gel method in the presence of a water-soluble organic polymer was tested in the reversed-phase acetonitrile–water linear gradient elution of polypeptides with molecular masses of up to 80 000. The silica rod having the through-pore size of 1.1  $\mu\text{m}$  and silica skeleton size of 0.7  $\mu\text{m}$  with mesopore size of 26 nm was used. The gradient time and the linear velocity of the mobile phase were varied and the resolution was examined in terms of peak capacity. The resolution with the silica rod was less affected by the gradient steepness and the mobile phase velocity. The results indicate that the silica rod column could reduce the separation time by a factor of 3 or more compared to the conventional column packed with 5  $\mu\text{m}$  silica particles. © 1998 Elsevier Science B.V. All rights reserved.

**Keywords:** Stationary phases; LC; Polypeptides; Silica rod column

### 1. Introduction

Gradient elution high-performance liquid chromatography (HPLC) has been widely used for separating peptides and proteins in reversed-phase, ion-exchange, hydrophobic-interaction and affinity modes. The diffusion coefficients of high-molecular-mass solutes in the pores of the packing materials are small, and the theoretical plate heights for such solutes depend much on the flow-rate of the mobile phase [1]. It is necessary to make the packing materials smaller and the pore size larger for separation in a short time. Recently, several kinds of materials have been proposed for the rapid separation in gradient elution HPLC by overcoming the prob-

lem of stagnant mobile phase mass transfer in porous packing materials.

Unger and co-workers reported that non-porous silica particles of diameter 1.5  $\mu\text{m}$  provided the rapid separation of proteins in reversed-phase mode [2,3]. Recently such materials have become available from several commercial sources. Perfusion chromatography using the polymer particles having through-pores of 600–800 nm and mesopores of 80–150 nm has been introduced by Afeyan and co-workers [4,5]. The through-pores, which allow the flow of mobile phase through the particles and effectively decrease the particle size, provided the high speed separation ability in ion-exchange and affinity modes. Hjerten and co-workers have developed the continuous separation media prepared by crosslinked polymer gel in a small diameter fused-silica tube [6–10]. Svec and co-workers have also developed the continuous

\*Corresponding author.

macro-porous rod separation media prepared by polymerizing monomers directly in a column [11–13]. The monolithic polymer gel columns were used successfully for high-speed separation of proteins and polypeptides in reversed-phase, ion-exchange, hydrophobic interaction, and affinity modes. Horvath and co-workers demonstrated that there was a significant advantage in separation speed and efficiency in working at elevated column temperatures up to 120°C with pellicular packing materials [14,15].

In previous papers, we reported the performance of continuous silica rod columns consisting of mesoporous silica skeletons and through-pores in isocratic elution [16–18]. The through-pore sizes and the silica skeleton sizes were varied from 1.0  $\mu\text{m}$  to 3.5  $\mu\text{m}$  independently from each other. The effects of the silica skeleton sizes and the domain sizes on the performance were evaluated for small molecules as well as insulin. The continuous silica rod columns with the smaller skeleton size or the domain size provided smaller plate heights and the less dependence on the mobile phase velocity than columns packed with 5  $\mu\text{m}$  particles. They also showed much lower back pressure than the particle-packed columns which had a similar theoretical plate height. It is of much interest to test the performance of a rod column with small-sized silica skeletons for the separation of high-molecular-mass solutes in gradient elution. This paper reports the use of an octadecylsilylated continuous silica rod column in reversed-phase gradient elution of polypeptides.

## 2. Experimental

### 2.1. Preparation of continuous porous silica column

A double-pore continuous silica rod was prepared according to the procedure described previously [15–17]. Tetramethoxysilane (TMOS: 40 ml, Tokyo Kasei, Tokyo, Japan) was added to 100 ml of 0.01 *M* aqueous acetic acid in the presence of 11.8 g of poly(ethylene oxide) (PEO, Aldrich, Milwaukee, WI, USA) with an average molecular mass of 10 000. The mixture was cooled in an ice bath and stirred for 30 min. The solution was poured into a polycarbonate mold (200×9 mm I.D.) and kept at 40°C for

gelation and aging for 15 h. The aged gel was immersed in 1.0 *M* aqueous ammonia solution at 120°C for 9 h. After drying at 50°C for three days, the monolithic gel was heat-treated at 700°C for 2 h. The continuous silica rod of 7.0 mm diameter was cut to 83 mm in length, encased in heat-shrinking PTFE tubing to be used in a Z-module (Waters, Milford, MA, USA) under external pressure, then octadecylsilylated by on-column reaction, as previously described [16–18].

A scanning electron microscopy system (SEM S-510, Hitachi, Japan) was employed for the observation of the morphology of the resultant gel. The domain size estimated from the SEM photographs was ca. 1.8  $\mu\text{m}$ . Characterization of the pore structure of the silica rod was performed by mercury porosimetry (PORESIZER 9320, Micromeritics, USA) and nitrogen adsorption method (ASAP 2000, Micromeritics) with an unmodified silica rod.

### 2.2. Chromatography

Chromatography was carried out using a conventional HPLC system consisting of two LC-10A pumps (Shimadzu, Kyoto Japan), an injection valve fitted with a 20- $\mu\text{l}$  sample loop (Model 7125, Rheodyne, Berkeley, CA, USA), an SPD-6A UV detector (Shimadzu) operated at 280 nm, and a data processor, V-Station, (GL Science, Tokyo, Japan). A conventional column packed with 5  $\mu\text{m}$  silica  $\text{C}_{18}$  particles, Capcellpak  $\text{C}_{18}$  SG, (150×4.6 mm I.D., Shiseido, Tokyo, Japan) with 30 nm pores was used for comparison. Furthermore, the separations were compared with several commercially available columns, 5  $\mu\text{m}$  silica  $\text{C}_{18}$  LiChrospher WP 300 RP-18e (125×4.0 mm I.D., Merck, Darmstadt, Germany) with 30 nm pores, 1.5  $\mu\text{m}$  nonporous silica  $\text{C}_{18}$ , NPS ODS-1 HPLC column (14×4.6 mm I.D., Micra Scientific, IL, USA), and 2.5  $\mu\text{m}$  nonporous polymer  $\text{C}_{18}$ , TSKgel Octadecyl-NPR (35×4.6 mm I.D., Tosoh, Yamaguchi, Japan). The NPS ODS-1 HPLC Column was tested with a specially designed HPLC instrument for a semi-micro column, NANOSPACE SI-1 (Shiseido). Mobile phase was prepared from LC-grade solvents. Chromatographic measurements were made at 30°C. A wide molecular-mass range of polypeptides (molecular mass in parentheses) from Sigma (St. Louis, MO, USA) were used,

glycyltyrosine (238), leucine enkephalin (556), insulin (6000), cytochrome *c* ( $12 \cdot 10^3$ ), lysozyme ( $14 \cdot 10^3$ ), transferrin ( $80 \cdot 10^3$ ), bovine serum albumin (BSA) ( $66 \cdot 10^3$ ),  $\beta$ -lactoglobulin ( $18 \cdot 10^3$ ) and ovalbumin ( $45 \cdot 10^3$ ). The samples were injected at the beginning of the solvent gradient, taking into account the gradient delay time due to the dwell volume. All gradient elution measurements were carried out using linear gradient [5–60% acetonitrile in the presence of 0.1% trifluoroacetic acid (TFA)]. In the gradient runs, the linear velocity of the mobile phase was varied at 1.0, 2.0, 3.0 and 4.0 mm/s and the gradient time was also varied from 3 to 30 min.

Recovery of polypeptides was examined by observing the peak areas of lysozyme, BSA and transferrin. The ratio of the average peak area of the three runs to the peak area obtained by replacing the column with a stainless steel tube ( $300 \times 0.3$  mm I.D.) was taken as the recovery.

### 3. Results and discussion

#### 3.1. The structure of the continuous porous silica

Fig. 1 shows the overall pore size distribution of the silica rod. The through-pore size was ca.  $1.1 \mu\text{m}$  with the pore volume of ca.  $4.2 \text{ cm}^3/\text{g}$ , and the mesopore size distributed at ca. 26 nm with the pore volume of  $0.98 \text{ cm}^3/\text{g}$ . The surface area was ca. 140

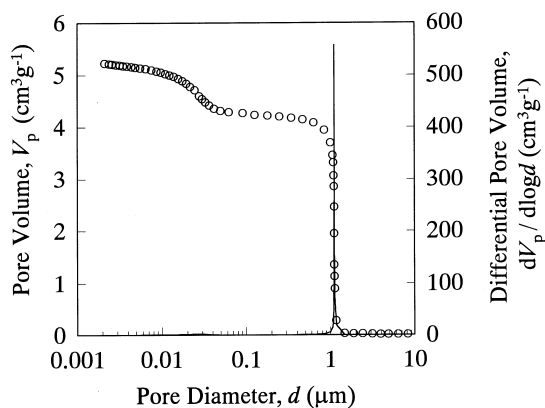


Fig. 1. Pore size distribution curve of the continuous silica rod. Pores larger than 100 nm were determined by mercury porosimetry and those smaller than 100 nm by nitrogen adsorption and the data were combined at  $d$  of 100 nm.

$\text{m}^2/\text{g}$ . The important feature in Fig. 1 is the large through-pore volume. From the size-exclusion chromatography (SEC) measurement, the through-pore volume of the rod column was found to be ca. 65% of the column volume, while the interstitial void volume in the conventional packed-column is commonly ca. 40% [19]. The continuous silica rod column was considered to be more loosely occupied by skeletons, resulting in much lower flow resistance, as reported previously [18]. Through-pore size (ca.  $1.1 \mu\text{m}$ ) is actually smaller than the size of interstitial voids in a column packed with  $5 \mu\text{m}$  particles.

#### 3.2. Performance of continuous porous silica column

The van Deemter plots obtained with amylobenzene as a solute in 80% methanol are shown in Fig. 2. Also shown are the plots with insulin in 30% acetonitrile for the silica rod and in 32% acetonitrile for Capcellpak  $\text{C}_{18}$  SG. The rod column gave much smaller plate heights and the slope of the plots than Capcellpak  $\text{C}_{18}$  SG. The results indicate that the column efficiency of the rod column is less affected by the mobile phase velocity than that of the column

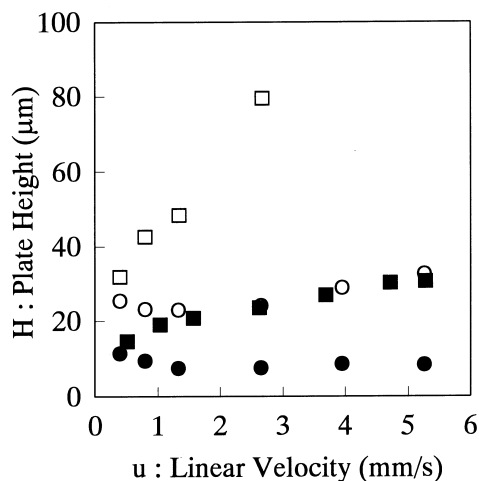


Fig. 2. Van Deemter plots for  $\text{C}_{18}$  silica rod (closed symbols) and Capcellpak  $\text{C}_{18}$  SG (open symbols) with amylobenzene (●, ○) and insulin (■, □) as solutes. Mobile phase: 80% methanol with amylobenzene and acetonitrile–water mixture with insulin (30:70, v/v) for rod column and (32:68, v/v) for Capcellpak  $\text{C}_{18}$  SG in the presence of 0.1% TFA.

packed with 5  $\mu\text{m}$  particles. Since the column length of the rod column and Capcellpak C<sub>18</sub> SG were 83 mm and 150 mm, respectively, both columns had similar theoretical plate numbers, which should play a major role in separation efficiency in gradient elution [20], while column length is considered to have little effect on resolution [21].

Fig. 3 shows the column back pressure against the linear velocity of the mobile phase. The back pressure per unit length of the rod column and Capcellpak C<sub>18</sub> SG were similar, thus the rod column provided the greater number of theoretical plates per unit pressure drop.

For isocratic measurements with acetonitrile–water mobile phase, retention can be approximated by Eq. (1) [22];

$$\log k' = \log k_0 - S\phi \quad (1)$$

where  $k'$  is the retention factor,  $k_0$  the value of  $k'$  in water as the mobile phase,  $\phi$  the volume fraction of acetonitrile in the mobile phase, and  $S$  a constant for a given compound. Fig. 4 shows the dependence of  $k'$  on  $\phi$  for some polypeptides in isocratic elution measurements. The rod column had smaller  $k'$  values than the particle-packed column at similar acetonitrile content. This is because the volume fraction and

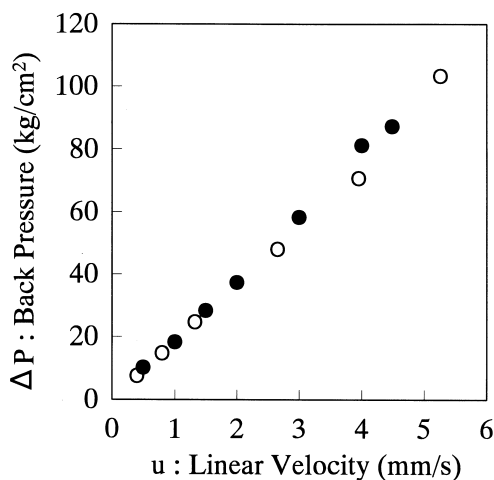


Fig. 3. Plots of column back pressure against linear velocity of mobile phase. Mobile phase: 80% methanol. The pressures were normalized to the column length of 83 mm. ●: Silica rod column.; ○ Capcellpak C<sub>18</sub> SG.

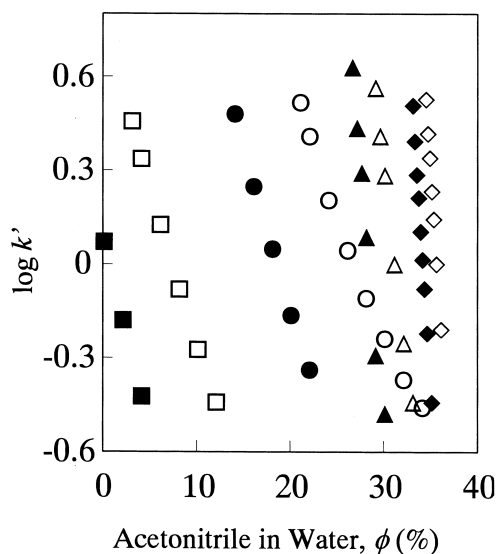


Fig. 4. Plots of the retention factor against the volume fraction of acetonitrile in mobile phase on silica rod column (closed symbols) and on Capcellpak C<sub>18</sub> SG (open symbols). ■, □: Glycyltyrosine, ●, ○: leucine-enkephalin, ▲, △: insulin, ◆, ◇: lysozyme.

the surface area of the silica skeleton in the rod column are much smaller than those of the silica particles in the packed column.

Stadalius and co-workers reported the relationship between the slope  $S$  and the molecular mass ( $M_r$ ) of the solutes in acetonitrile–water mobile phase as Eq. (2) [23];

$$S = 0.48 (M_r)^{0.44} \quad (2)$$

The plots of  $\log S$  values against  $\log (M_r)$  on the rod column and Capcellpak C<sub>18</sub> SG are shown in Fig. 5, where the  $S$  values with leucine enkepharin and insulin were obtained from Fig. 4 and those with BSA and ovalbumin were calculated from the retention data obtained at different gradient time measurements [23]. The following relationships were derived from the plots in Fig. 5.

$$S = 0.71 (M_r)^{0.45} \quad (3)$$

$$S = 0.58 (M_r)^{0.45} \quad (4)$$

The coefficient in the equation for the rod column (Eq. (3)) was ca. 20% larger than that for Capcellpak

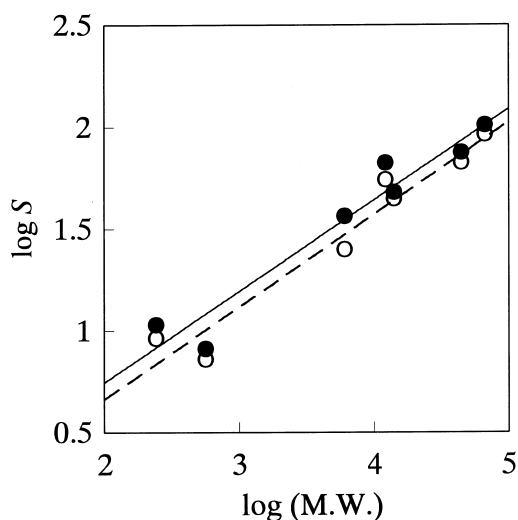


Fig. 5. Plots of  $S$  values against molecular mass of polypeptide. ●: Silica rod column, ○: Capcellpak  $C_{18}$  SG. Solid line corresponds to the best fit to data points for the rod column and dashed line for Capcellpak  $C_{18}$  SG.

$C_{18}$  SG (Eq. (4)). This is presumably due to the lower coverage of the silica surface of the rod column than Capcellpak  $C_{18}$  SG, which agreed with the lower hydrophobic selectivity,  $\alpha(\text{CH}_2)$ , of the  $C_{18}$  silica rod than a column packed with porous  $C_{18}$ -silica particles, as reported previously [17]. The results indicate that the band spacing would be slightly narrower on the rod column than with a conventional column packed with porous silica  $C_{18}$  particles under similar gradient conditions. However, high-performance of the silica rod shown in Fig. 2 and the complete recovery of the polypeptides, shown in Table 1, suggest that the octadecylsilylated silica rod column is suitable for the separation of polypeptides.

Fig. 6 shows the comparison between the rod column and Capcellpak  $C_{18}$  SG in gradient elution of

Table 1  
Recovery of polypeptides

Polypeptide	Recovery (%)	
	Rod column	Capcellpak $C_{18}$ SG
Lysozyme	100	100
BSA	96	88
Transferrin	102	100

polypeptides. The difference in the column diameter is considered to have little effect on resolution in gradient elution [21]. At the mobile phase velocity of 2 mm/s, baseline separation could be achieved with 10 min gradient time,  $t_G$ , on the rod column. On the other hand, it took much longer time for Capcellpak  $C_{18}$  SG to achieve similar separation. Comparing the chromatogram of  $t_G=5$  min on the rod column to that of  $t_G=15$  min on Capcellpak  $C_{18}$  SG, the rod column seemed to give better separation. These results indicate that the silica rod column can be used with steeper gradient than the conventional column packed with 5  $\mu\text{m}$  silica particles, which results in the reduction in not only the separation time but also the consumption of the mobile phase by a factor of 3 or more by employing a column of a similar size.

The resolution in gradient elution can be compared in terms of peak capacity, PC, which indicates the maximum number of peaks that can be fitted into the chromatogram with unit resolution. The peak capacity is defined by Eq. (5) [23];

$$\text{PC} = t_G / 4\sigma_t \quad (5)$$

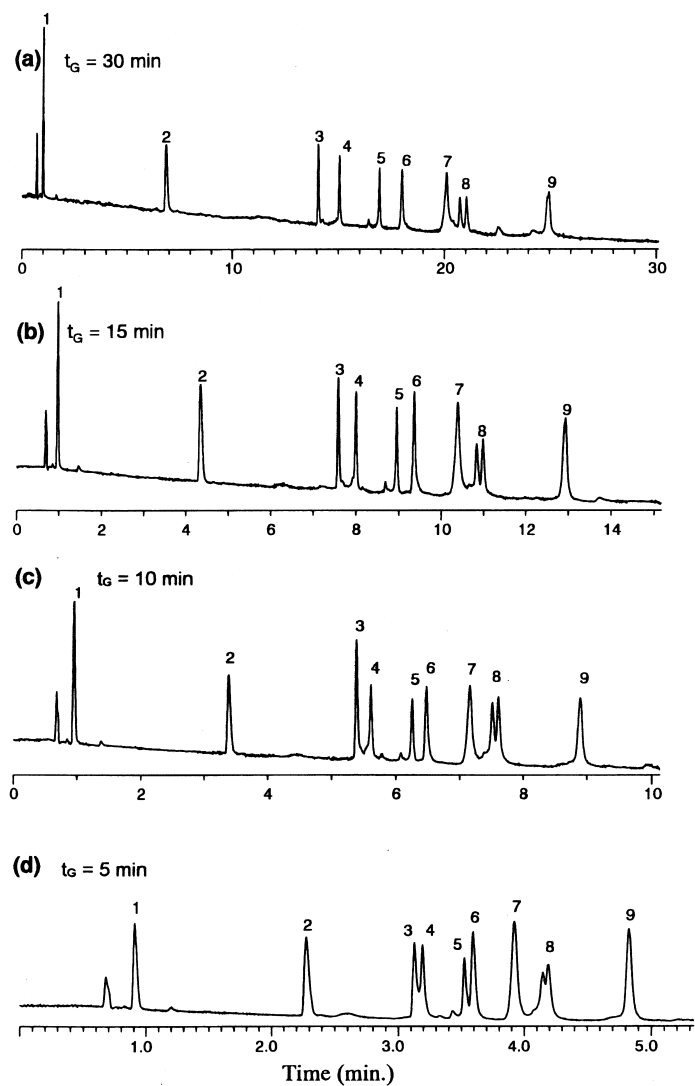
where  $t_G$  is the gradient time and  $4\sigma_t$  the band width in time unit. Fig. 7 shows the plots of peak capacity against the gradient steepness parameter,  $b$ . The parameter  $b$  is defined by Eq. (6) [22] and can be calculated by Eq. (7) from the retention times at two different gradient times [23];

$$b = St_0 \Delta\phi / t_G \quad (6)$$

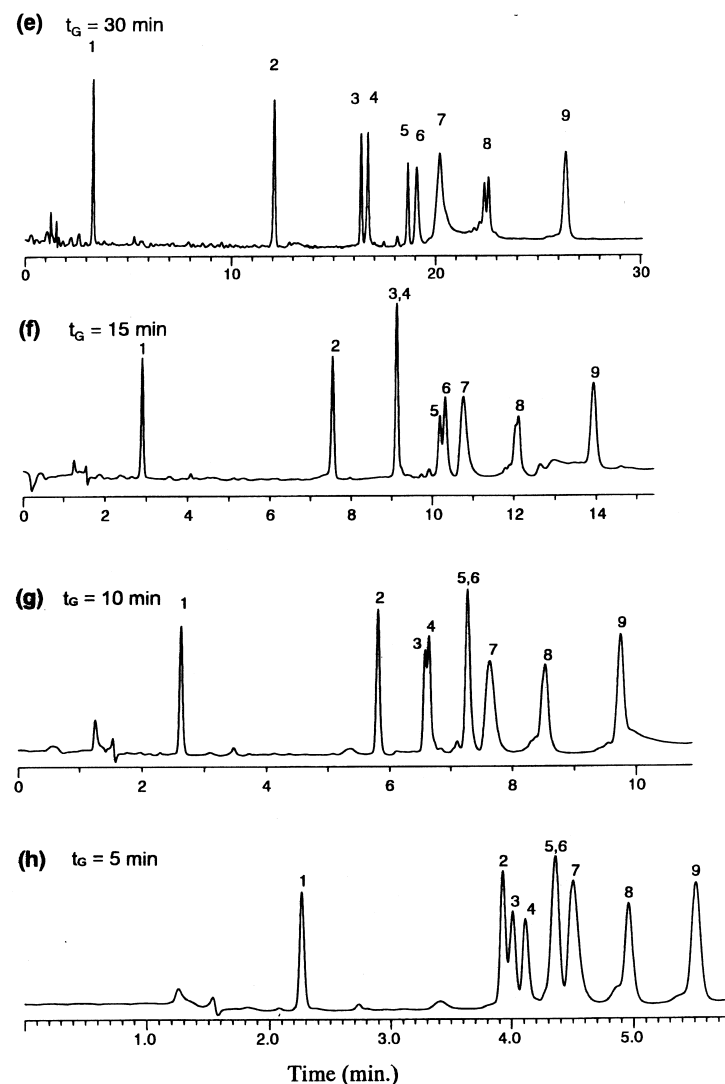
$$b = t_0 \log \beta / [t_{g1} - (t_{g2}/\beta) + t_0(1 - \beta)/\beta] \quad (7)$$

where  $\Delta\phi$  is the change in volume fraction of the organic solvent during the gradient run,  $t_{g1}$ ,  $t_{g2}$  the gradient retention times,  $\beta = t_{g2}/t_{g1}$ , and  $t_0$  the elution time of uracil. For leucine enkephalin there was small difference in PC between the two columns, Capcellpak  $C_{18}$  SG being slightly better than the rod column, as shown in Fig. 7a. However, the rod column showed much better resolution than Capcellpak  $C_{18}$  SG with polypeptides of high molecular mass, as shown in Fig. 7b–d.

Fig. 7 includes the plots of PC at the mobile phase velocity of 1–4 mm/s. The PC with the rod column was little affected by the mobile phase



### Silica rod column



### Capcellpak C<sub>18</sub> SG

Fig. 6. Elution of polypeptides [(1)glycyltyrosine; (2) leucine-enkephalin; (3) insulin; (4) cytochrome *c*; (5) lysozyme; (6) transferrin; (7) BSA; (8)  $\beta$ -lactoglobulin; (9) ovalbumin] on silica rod column (a, b, c and d) and Capcellpak C<sub>18</sub> SG (e, f, g and h). Linear gradient from 5 to 60% acetonitrile in the presence of TFA at 2 mm/s of mobile phase velocity. Gradient time: 30 min (a and e), 15 min (b and f), 10 min (c and g), 5 min (d and h).

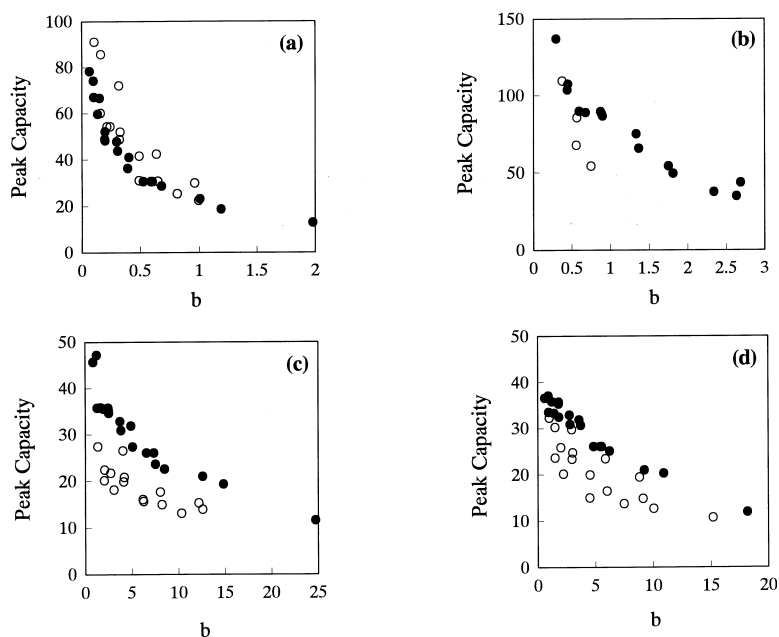


Fig. 7. Plots of peak capacity against gradient steepness. ●: silica rod column, ○: Capcellpak C<sub>18</sub> SG. Polypeptide: leucine-enkephalin (a), insulin (b), BSA (c) and ovalbumin (d).

velocity, while the PC values for the late-eluting peptides with Capcellpak C<sub>18</sub> SG showed a decrease with the increase in the mobile phase velocity. These results indicate that the silica rod column can be applied for the separation of high molecular weight samples at the greater gradient steepness.

Fig. 8 shows the comparison among the rod column and the columns packed with several high-performance particles at the mobile phase velocity of 4 mm/s and the gradient time of 5 min. The nonporous particles, 1.5 μm silica-based NPS (Fig. 8d) and 2.5 μm polymer-based NPR (Fig. 8e) showed much shorter retention and considerably different selectivity for the polypeptides. High efficiency was observed for early-eluting polypeptides with the 1.5 μm particles. The separation efficiency of the rod column is shown to be similar to or higher than that of the small non-porous particles and much higher than that of the conventional 5 μm particles. The high efficiency of the rod column is presumably provided by the small-sized silica skeletons which resulted in a much smaller increase in plate height

with the increase in the flow-rate of the mobile phase (Fig. 2).

#### 4. Conclusions

The continuous porous silica column having 0.7 μm silica skeletons and 1.1 μm through-pores showed much higher separation efficiency, especially under a steep gradient, for polypeptides than the conventional columns packed with 5 μm wide-pore silica particles in reversed-phase gradient elution in acetonitrile–water in the presence of TFA. Under the same gradient elution conditions, the continuous silica rod column provided nearly equal or higher efficiency at much lower pressure drop compared to the column packed with 1.5–2.5 μm particles.

#### Acknowledgements

This work was supported in part by a Grant-in-Aid

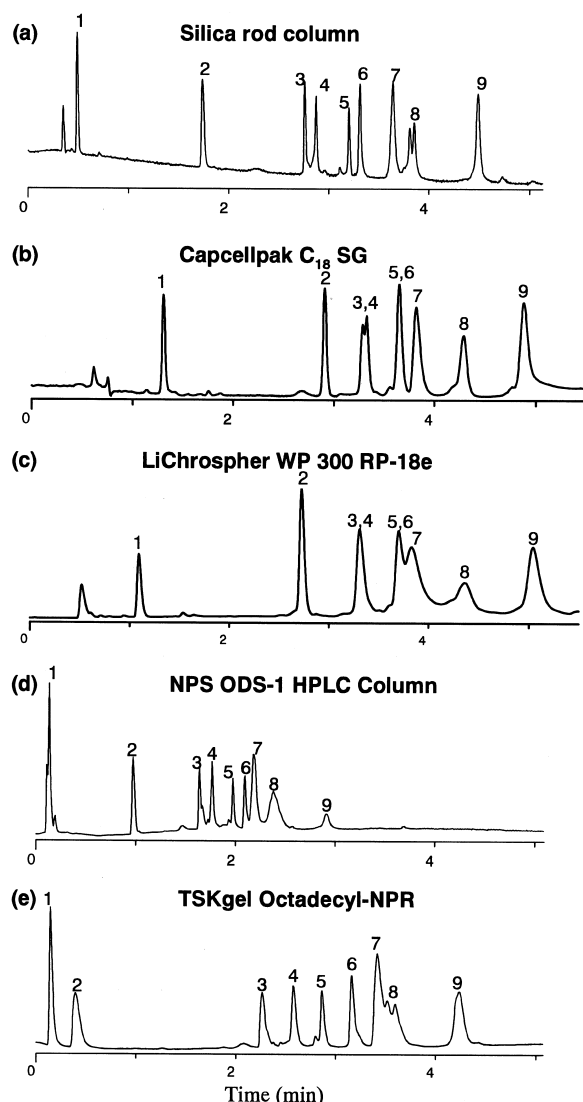


Fig. 8. Elution of polypeptides on silica rod column and particle packed columns. Solute as in Fig. 6. Mobile phase velocity: 4 mm/s. Gradient: 5 to 60% acetonitrile in the presence of TFA. Gradient time: 5 min. Column: silica rod column (a), Capcellpak C<sub>18</sub> SG (b), LiChrospher WP 300 RP-18e (c), NPS ODS-1 HPLC Column (d), and TSKgel Octadecyl-NPR (e).

for Scientific Research from the Ministry of Education, Science, Sports and Culture.

## References

- [1] J.C. Giddings, *Dynamics of Chromatography, Part 1, Principles and Theory*, Marcel Dekker, New York, 1965.
- [2] K.K. Unger, G. Jilge, J.N. Kinkel, M.T.W. Hearn, *J. Chromatogr.* 359 (1986) 61–72.
- [3] K.K. Unger, G. Jilge, R. Janzen, H. Giesche, *Chromatographia* 22 (1986) 379–380.
- [4] N.B. Afeyan, N.F. Gordon, I. Mazsaroff, L. Varady, Y.B. Yang, F.E. Regnier, *J. Chromatogr.* 519 (1990) 1–29.
- [5] N.B. Afeyan, S.P. Fulton, F.E. Regnier, *J. Chromatogr.* 544 (1991) 267–279.
- [6] J.L. Liao, S. Hjerten, *J. Chromatogr.* 457 (1988) 165–174.
- [7] S. Hjerten, J.L. Liao, R. Zhang, *J. Chromatogr.* 473 (1989) 273–275.
- [8] S. Hjerten, K. Nakazato, J. Mohammad, D. Eaker, *Chromatographia* 37 (1993) 287–294.
- [9] Y.-M. Li, J.-L. Liao, K. Nakazato, J. Mohammad, L. Terenius, S. Hjerten, *Anal. Biochem.* 223 (1994) 153–158.
- [10] C. Ericson, J.-L. Liao, K. Nakazato, S. Hjerten, *J. Chromatogr.* 767 (1997) 33–41.
- [11] F. Svec, J.M.J. Frechet, *Anal. Chem.* 64 (1992) 820–822.
- [12] Q.C. Wang, F. Svec, J.M.J. Frechet, *Anal. Chem.* 65 (1993) 2243–2248.
- [13] Q.C. Ching, F. Svec, J.M.J. Frechet, *J. Chromatogr. A* 669 (1994) 230–235.
- [14] F.D. Antia, C. Horvath, *J. Chromatogr.* 435 (1988) 1–15.
- [15] C. Chen, C. Horvath, *Anal. Methods Inst.* 1 (1993) 213–222.
- [16] H. Minakuchi, K. Nakanishi, N. Soga, N. Ishizuka, N. Tanaka, *Anal. Chem.* 68 (1996) 3498–3501.
- [17] H. Minakuchi, K. Nakanishi, N. Soga, N. Ishizuka, N. Tanaka, *J. Chromatogr. A* 762 (1997) 135–146.
- [18] H. Minakuchi, K. Nakanishi, N. Soga, N. Ishizuka, N. Tanaka, *J. Chromatogr. A* 797 (1998) 121–131.
- [19] K.K. Unger, *Porous Silica*, Elsevier, Amsterdam, 1979.
- [20] J.W. Dolan, J.R. Gant, L.R. Snyder, *J. Chromatogr.* 165 (1979) 31–58.
- [21] W.G. Burton, K.D. Nugent, T.K. Slattery, B.R. Summers, L.R. Snyder, *J. Chromatogr.* 443 (1988) 363–379.
- [22] L.R. Snyder, in: C. Horvath (Ed.), *High-Performance Liquid Chromatography, Vol. 1*, Academic Press, New York, 1980.
- [23] M.A. Stadalius, H.S. Gold, L.R. Snyder, *J. Chromatogr.* 296 (1984) 31–59.